

Some Effects of Surface Anomalies in a Global General Circulation Model¹

JEROME SPAR—Department of Meteorology and Oceanography,
New York University, New York, N.Y.²

ABSTRACT—The Mintz-Arakawa two-level general circulation model has been used in a series of experiments to compute the response of the atmosphere to certain persistent sea-surface temperature anomalies and to changes in the position of the continental Northern Hemisphere snow line over periods up to 90 days. Results are shown in terms of differences between anomaly and control histories as revealed by global, 30-day mean sea-level pressure maps and time series of three regional indices of synoptic activity. The experiments show significant interhemispheric effects after about 1 mo, phase shifts of 1–2 weeks in major cyclone developments, stronger reactions to sea-temperature anomalies in winter than in summer, and marked influence of the snow line on the winter monsoonal pressure difference between the continents and the North Atlantic Ocean.

1. INTRODUCTION

The development of several realistic and computationally stable general circulation models (e.g., Mintz 1965, Smagorinsky et al. 1965, Leith 1965, Kasahara and Washington 1967, Holloway and Manabe 1971) appears to have opened the way for some preliminary experimentation in dynamical long-range weather prediction. Although a direct operational attack on the long-range forecasting problem by extended time integrations of general circulation models cannot be seriously proposed at this time, the models may be expected to provide at least tentative answers to certain basic questions related to long-range weather forecasting.

For many years, meteorologists have sought a physical basis for long-range weather prediction. Several workers in the field have hypothesized that certain anomalous surface conditions force long-term responses in the atmosphere. For example, anomalies in sea ice, snow cover, and sea-surface temperature have been suggested as possible causes of subsequent atmospheric anomalies. In a series of papers published over the past decade, Namias (1962, 1969, 1971) has noted the occasional persistence of large sea-surface temperature (SST) anomalies and has speculated on their possible influence on the atmosphere over months, seasons, and even years. Similar views have also been put forth by Bjerknes (1966, 1969), particularly with respect to possible remote effects of SST anomalies in the equatorial Pacific.

Because of the strong interactions between the atmosphere and the earth's surface, long-range weather prediction must eventually seek to account for the variations in the coupled earth-atmosphere system over the forecast period. [The joint ocean-atmosphere general circulation model of Manabe and Bryan (1969) represents the first

significant attempt to deal with this problem.] As Namias (1970) has noted, however, sea-surface temperature anomalies, once established, may persist for a long time thereafter, despite interactions with the atmosphere. In such cases, it may be possible to calculate the effects of these persistent anomalies on the subsequent behavior of the atmosphere even with a noninteractive model.³

A set of experiments has been carried out at the Goddard Institute for Space Studies (GISS) with the global, two-level, general circulation model developed by Y. Mintz and A. Arakawa at the University of California in Los Angeles (UCLA). (See references in sec. 2.) In these experiments, certain hypothetical anomalies in sea temperature and snow cover were introduced, and the model was run for periods up to 3 mo. The response of the model atmosphere to the anomalous surface conditions was evaluated by comparing these "anomaly" runs with "control" runs based on identical conditions except for the absence of the surface anomalies.

It must be emphasized that these experiments do not bear directly on the problem of the inherent predictability of the atmosphere. Predictability experiments (e.g., National Academy of Sciences 1966) have clearly demonstrated that model predictions started from two initial states that differ by only a small random error field soon diverge, and that the two predicted fields may become uncorrelated after about 2 weeks. Thus, the effects of random error, or of random variation in initial state, may completely overwhelm any effects due to systematic anomaly fields such as those studied here. Obviously, one cannot expect to predict the future state of the atmosphere any more reliably when surface anomalies are present than when they are absent. The purpose of these numerical

³ Rowntree (1972) has published an account of an experiment conducted in 1968 with the nine-level hemispheric model developed at the Geophysical Fluid Dynamics Laboratory (Smagorinsky et al. 1965) in which he attempted to verify Bjerknes' (1966) hypothesis concerning the influence of anomalies in the tropical Pacific Ocean on pressure and circulation patterns in higher latitudes. While no direct comparison of the present study with Rowntree's experiment is possible, the general conclusions regarding the importance of sea-air energy exchanges and the far-reaching influence of sea-surface temperature anomalies are similar.

¹ The research reported in this paper was supported by the Goddard Space Flight Center, NASA, under Grant NGR 33-016-174 and was begun during the summer of 1971 while the author was a National Research Council Senior Research Associate at the Goddard Institute for Space Studies in New York.

² Contribution No. 131, Geophysical Sciences Laboratory, New York University

experiments is only to determine what the specific contributions of the anomalies studied may be to the total variability of the atmosphere.

2. GENERAL CIRCULATION MODEL

The two-level model originally devised by Mintz (1965) has undergone a series of modifications and is now in the form described by Langlois and Kwok (1969), but with the treatment of radiation and convection as given by Arakawa et al. (1969). A full description of the model can be found in Gates et al. (1971).

In brief, the model atmosphere, bounded below by the earth's surface and above by the 200-mb level, is divided into two layers of equal mass. The horizontal wind velocities and temperatures of the two layers, the water vapor in the lower layer, and the surface pressure are predicted using the primitive equations cast in "sigma" coordinates on a spherical grid of 5° of longitude by 4° of latitude. [The vertical coordinate, σ , is defined as the ratio, $(p - p_T)/(p_s - p_T)$, where p is pressure, p_T is pressure at the top (i.e., 200 mb), and p_s is the surface pressure.] Geopotential heights and pressures of σ surfaces are computed diagnostically and converted to geopotential heights of isobaric surfaces. The earth's surface is specified as open ocean with a given surface temperature distribution, or as bare land of given altitude, or as ice-covered ocean or ice- or snow-covered land. Except for the temperature and soil moisture of bare land, surface conditions are not predicted by the model. The model includes a water cycle (with clouds and precipitation), a parameterized moist convection scheme, infrared and solar radiation fluxes (including continuously varying solar distance, declination, and zenith angle), variable ground temperature (computed from a surface energy balance condition), and a prescribed seasonal variation in the latitude of the snow line (i.e., the southern edge of the snow cover) over the continents in the Northern Hemisphere.

The control runs with the model were computed using a fixed climatological mean annual sea-surface temperature field and a snow line that oscillates sinusoidally with time from a minimum latitude of 45°N (in January) to a maximum of 75°N (in July). As shown by Mintz et al. (1972), this model, starting from a state at rest, generates a credible meteorological history, including a realistic climatology and annual cycle.

3. EXPERIMENTS AND MEASURES OF RESPONSE

Simulated predictions were computed for both the summer and winter seasons. In each experiment, the run begins with the solar declination set close to its maximum or minimum value, depending on the season. Both declination and solar distance, as well as zenith angle, are then allowed to vary appropriately with calendar date during the 3-mo forecast run. Initial conditions for each season were taken from the history tapes generated by the model at UCLA from a state of rest. Although they were picked at random from the UCLA history tapes, the initial conditions for each experiment are characteristic

of the given season, and in every case the solar declination was set initially at its appropriate solstitial value.⁴

In the experiments identified as NHTA (Northern Hemisphere sea-surface Temperature Anomaly), a positive anomaly of 2° – 6°C was added to the mean annual sea-surface temperature over a "box" in the North Pacific Ocean between latitudes 22° – 42°N and longitudes 140°W – 180° . The anomaly on the perimeter gridpoints of the box was set at 2°C , increasing to 4°C at points one gridpoint in from the perimeter, and to a maximum of 6°C at points two gridpoints in from the perimeter; that is, along 30° – 34°N and 150° – 170°W . This SST anomaly pattern was suggested by the 1968 SST anomaly field in the North Pacific as described by Namias (1971). However, it was not the purpose of this study to attempt to simulate the sequence of events discussed by Namias. The initial state for the model experiments does not correspond to that of the 1968 case, and, even if it did, the model could not be expected to simulate the observed meteorological history with high fidelity. The same SST anomaly was used for both the summer and winter experiments, which are designated NHTA-S and NHTA-W, respectively.

A third SST anomaly experiment was carried out by introducing the same positive anomaly pattern in the South Pacific Ocean, between latitudes 22° – 42°S and longitudes 140°W – 180° . For this experiment, the initial conditions selected were those of the initial Northern Hemisphere summer (Southern Hemisphere winter) day. This experiment, which is designated SHTA (Southern Hemisphere sea-surface Temperature Anomaly), was undertaken following the discovery that significant effects of the NHTA appeared in the opposite hemisphere after about 1 mo.

The fourth experiment, described later in this paper, was conducted to evaluate the response of the atmosphere to an anomalous snow cover. Designated SNW, this experiment consisted of shifting the mean latitude of the specified continental Northern Hemisphere snow line either 5° north (SNW-N) or 5° south (SNW-S). The minimum latitude of the snow line thus becomes 50°N in SNW-N and 40°N in SNW-S. Both these experiments were performed only for the winter season and were intended to provide some insight into the seasonal response of the atmosphere to the anomalous albedo and heat exchange associated with anomalies in snow cover.

The response of the model atmosphere to the surface anomalies was examined mainly in terms of global maps of monthly mean sea-level pressures and time series of three regional indices of synoptic activity. The P-index is a daily space-time average sea-level pressure (mb) computed over the eastern region of North America bounded by latitudes 30° and 50°N and longitudes 70° and 90°W . It is evaluated by averaging 2-hourly values of sea-level pressures over 30 gridpoints each day. The Z-index is a daily geostrophic zonal circulation index at 600 mb for a zonal belt extending across North America from longitude 50° – 140°W between latitudes 30° and 50°N .

⁴ The initial solar calendar dates corresponding to the summer and winter experiments, respectively, were actually June 17 and December 20.

It is equal to the meridional difference in daily mean 600-mb geopotential height (m) across the latitude band; positive values of Z represent geostrophic westerly winds. The M-index is a daily geostrophic meridional circulation index at 600 mb over the eastern region of North America and is defined as the zonal difference in daily mean geopotential height between longitudes 70° and 90° W over the latitude band from 30° to 50° N. Positive values of M denote southerly geostrophic winds, and ridge or trough passages at 600 mb are indicated by reversals in the sign of M .

4. RESULTS OF EXPERIMENTS

In each experiment, monthly mean sea-level pressure maps and 90-day time series of the three regional indices were computed for both the anomaly run and the corresponding control run. Difference maps and difference time series were also computed for each pair of anomaly and control runs, and the results of the experiments are discussed mainly in terms of these differences between the anomaly and control histories. In the interests of brevity, however, only a few of the more interesting results are reviewed in this paper. For example, the response to an SST anomaly in the summer hemisphere, as represented by NHTA-S, was generally slower, weaker, and less systematic than that associated with the same anomaly in the winter hemisphere, as represented, for example, by NHTA-W, although qualitatively there were similarities between the two seasons. Therefore, only the winter experiments are illustrated and discussed here. Additional details on all the experiments may be found in Spar (1972).

NHTA-W

The 30-day mean sea-level pressure fields for the control and anomaly runs, as well as the difference fields (anomaly minus control) for each month of this experiment are shown in figures 1-3. The isobars were drawn by computer at 5-mb intervals.

In the first month (fig. 1), the effects of the SST anomaly are observed only in the Northern Hemisphere and mainly to the northeast of the SST anomaly area. For example, the cyclone in the Gulf of Alaska is deeper and the North Atlantic Low is weaker on the anomaly map than on the control map. In the second month (fig. 2), however, the pressure differences in the Gulf of Alaska virtually disappear with the development of a very deep North Pacific cyclone on both anomaly and control maps. Now the principal effects are seen in the North Atlantic and in the Southern Hemisphere. On the anomaly map, the North Atlantic cyclone is west of its position on the control map, while in the Southern Hemisphere the pressure gradient is reversed across the southern tip of South America.

The principal differences are again found in the same regions in the third month (fig. 3). At this time, the anomaly map exhibits a stronger Greenland High and a deeper Atlantic Low than the control map does, as shown by the large pressure gradient south of Greenland on the

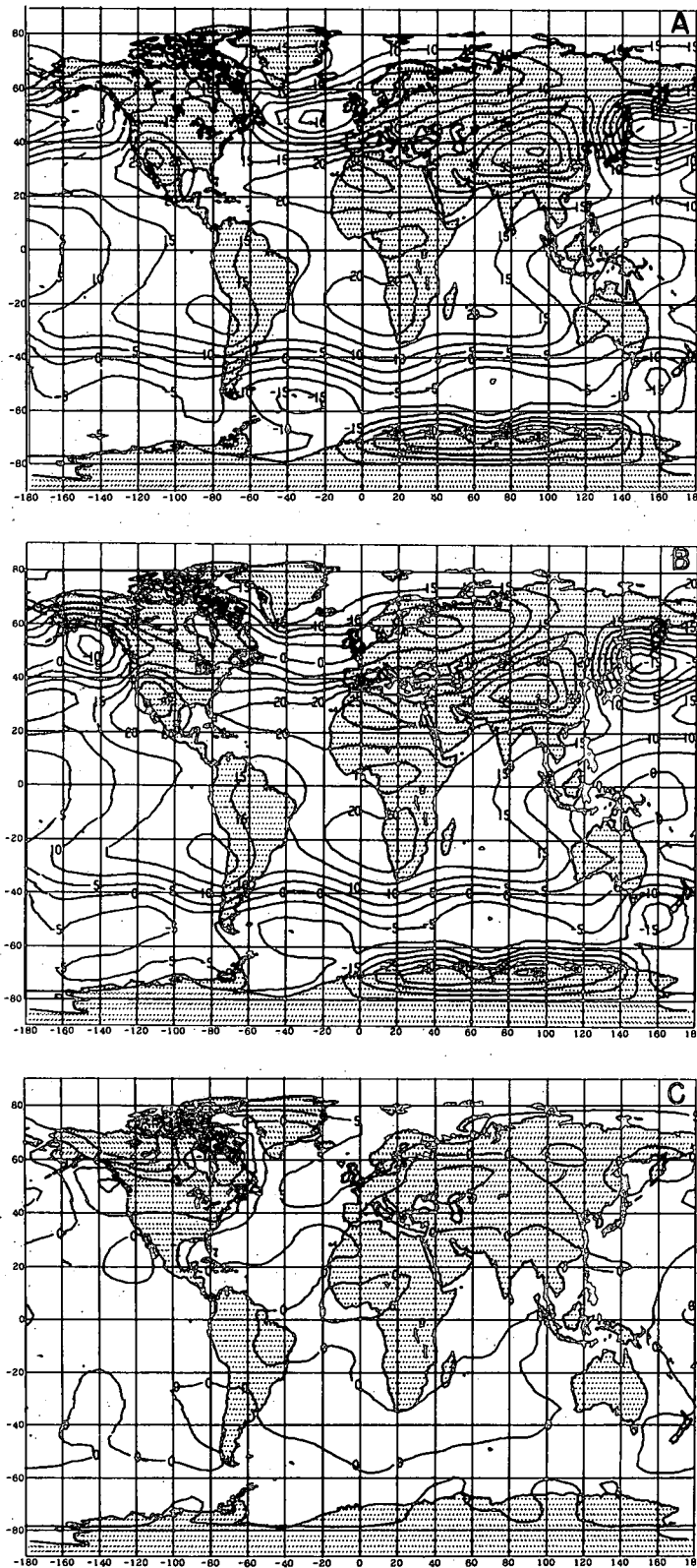


FIGURE 1.—Thirty-day mean sea-level (A) control, (B) anomaly, and (C) anomaly minus control pressure maps for month number 1 (1-30 days) of experiment NHTA-W. Isobars are drawn for every ± 5 mb.

difference map (fig. 3C). The effect of the North Pacific SST anomaly on the sea-level pressure field in the Southern Hemisphere in the third month takes the form of weaker westerlies on the anomaly map than on the control map. With pressures on the anomaly map higher in the sub-

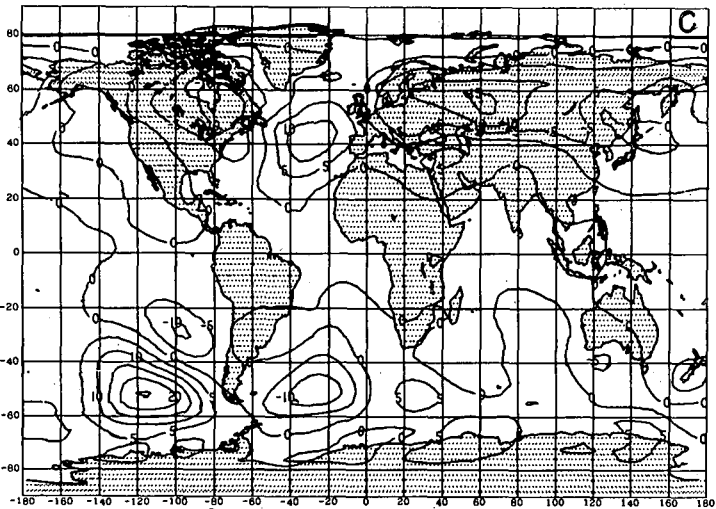
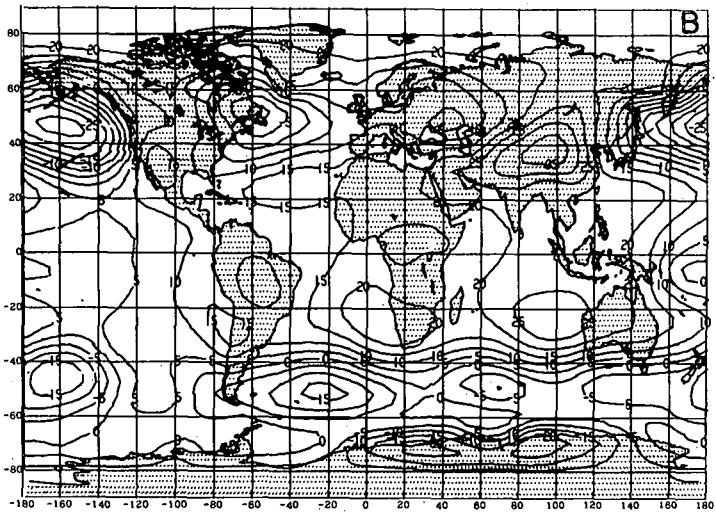
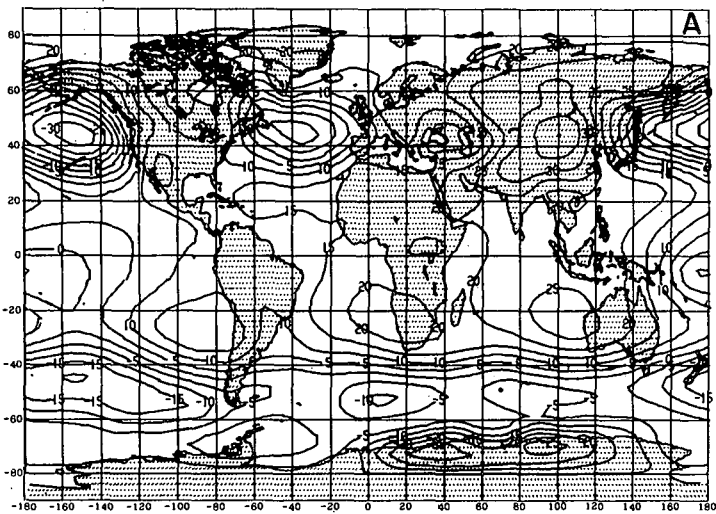


FIGURE 2.—Same as figure 1 for month number 2 (31-60 days).

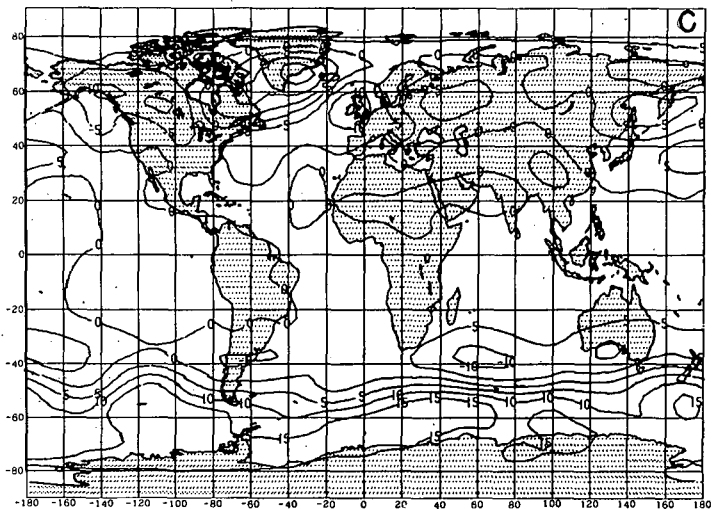
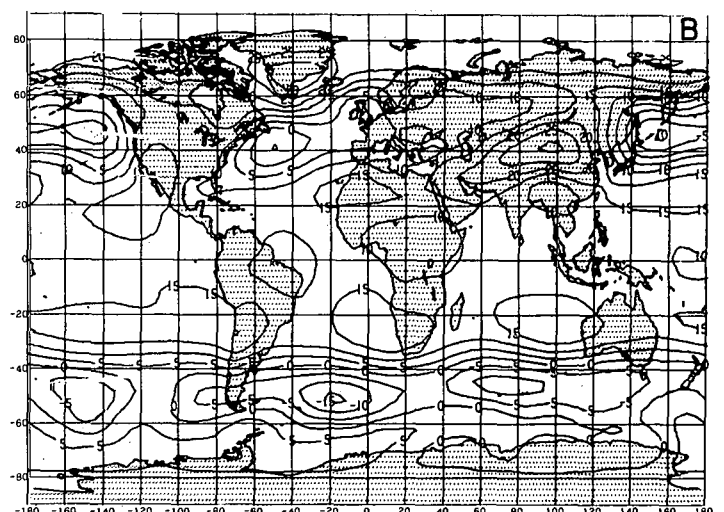
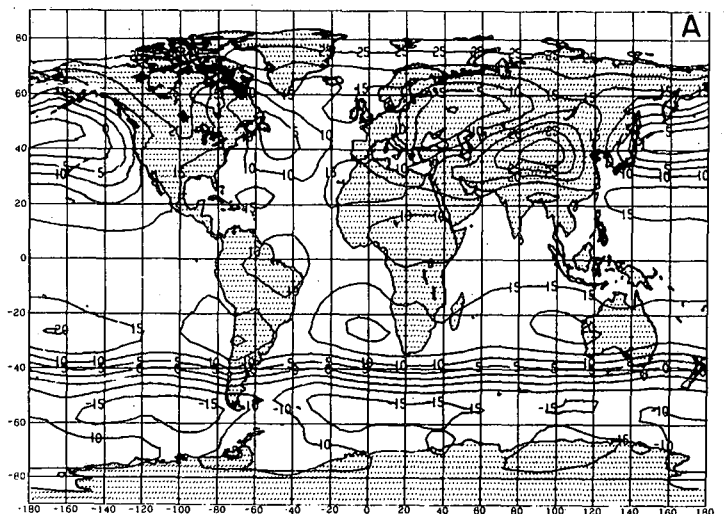


FIGURE 3.—Same as figure 1 for month number 3 (61-90 days).

antarctic low-pressure belt and lower in the Southern Hemisphere subtropical high-pressure belt than on the control map, the meridional sea-level pressure gradient in middle latitudes of the Southern Hemisphere is significantly weakened by the SST anomaly in the opposite

hemisphere. It is noteworthy that this influence appears to cross the Equator without producing any visible effect on the sea-level pressure field at the Equator itself.⁵

⁵ Further studies of transequatorial propagation in the model experiments will be described in a later publication.

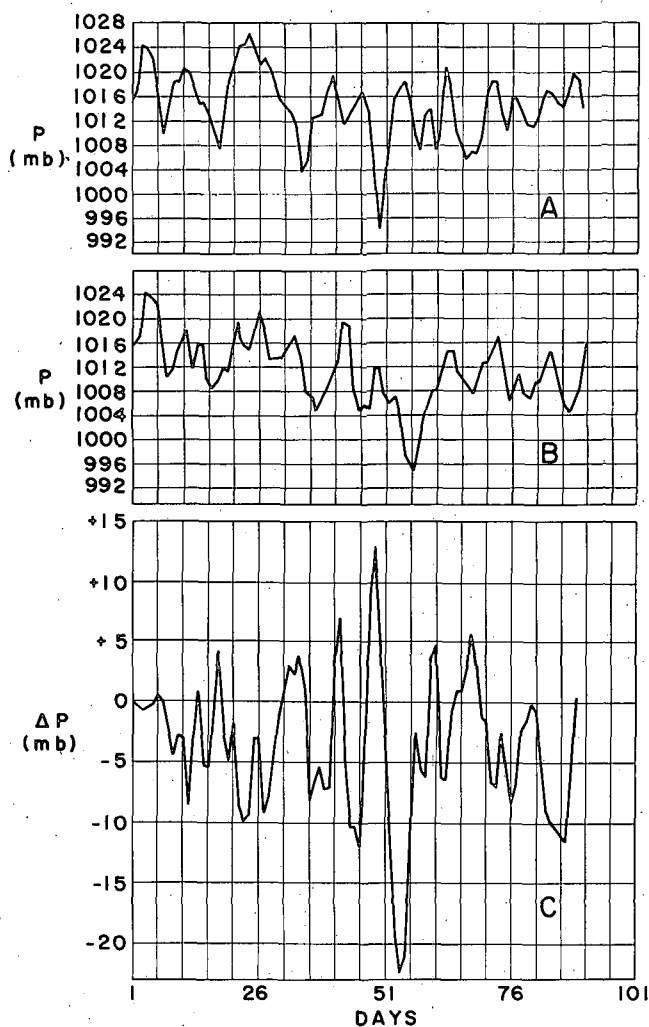


FIGURE 4.—Ninety-day time series of North American east coast sea-level pressure index, P (mb), for the (A) control, (B) anomaly, and (C) anomaly minus control runs of experiment NHTA-W.

Some regional effects of the SST anomaly are illustrated by the time series of the three regional indices, P (fig. 4), Z (fig. 5), and M (fig. 6). Significant differences in P between anomaly and control do not begin to appear on the east coast until about 6 days after starting time. The amplitude of the P -difference curve (fig. 4C) then increases with time to a maximum of 13 mb on day 49. This maximum difference is primarily the result of a phase delay of 6 days in the major cyclonic event of the season on the east coast of North America, as seen in figures 4A and 4B. In both the anomaly and control histories, a minimum of about 994 mb in the space-time averaged sea-level pressure develops in the east coastal region. This minimum, however, arrives almost a week later in the anomaly case than in the control case. In general, the SST anomaly apparently neither generates nor suppresses cyclonic events, but it may alter their phase. Power spectra (not shown) of the P -series indicate only slightly greater variance in the anomaly spectrum, compared with the control, at the highest and lowest frequencies, and a marked reduction in variance over all periods between 3

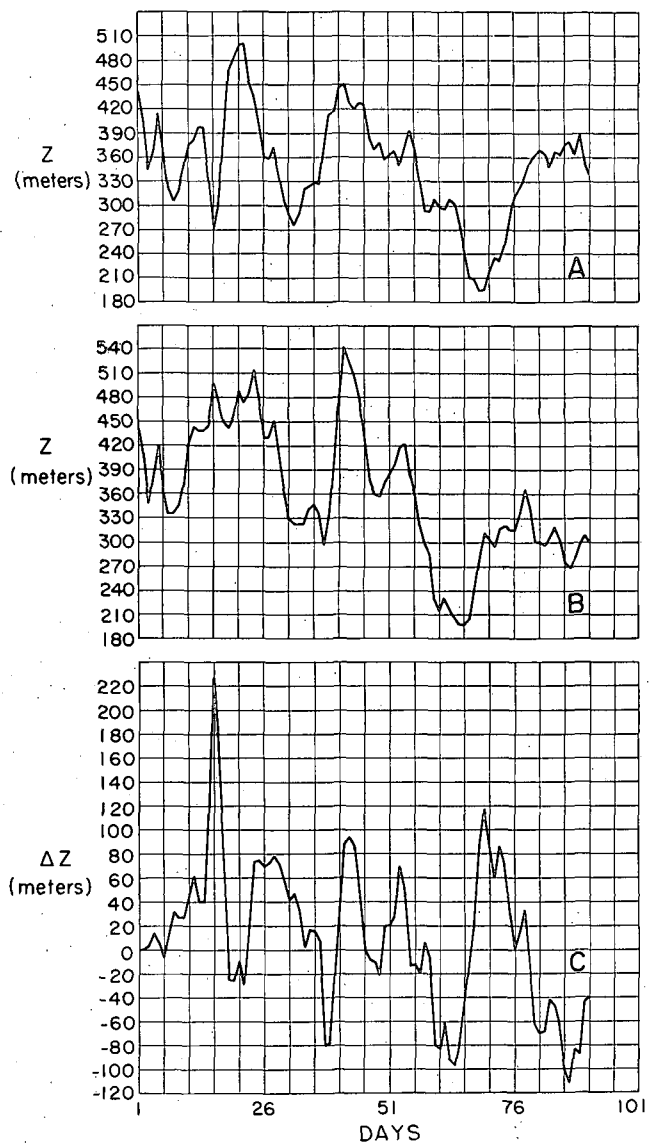


FIGURE 5.—Same as figure 4 for the 600-mb regional zonal index, Z (m).

and 10 days. This also suggests that the SST anomaly does not contribute to increased sea-level synoptic activity, at least in the eastern United States.

The two 90-day time series of the 600-mb Z -index for experiment NHTA-W (fig. 5) indicate no systematic effect of the SST anomaly after a large initial increase in Z during the first month. The maximum difference of more than 220 m (equivalent to a geostrophic wind difference of about 10 m/s), which appears on day 16, probably reflects the effect of an enhanced meridional temperature gradient in the lower troposphere between latitudes 30° and 50° N resulting from the SST anomaly maximum at 32° N. A similar increase in Z was found in the NHTA-S experiment (not shown). In the summer experiment, however, the Z -index difference continues to increase with time during the 3-mo period, while in the winter experiment the rise appears to be a transient phenomenon that disappears after about a half month. Apparently,

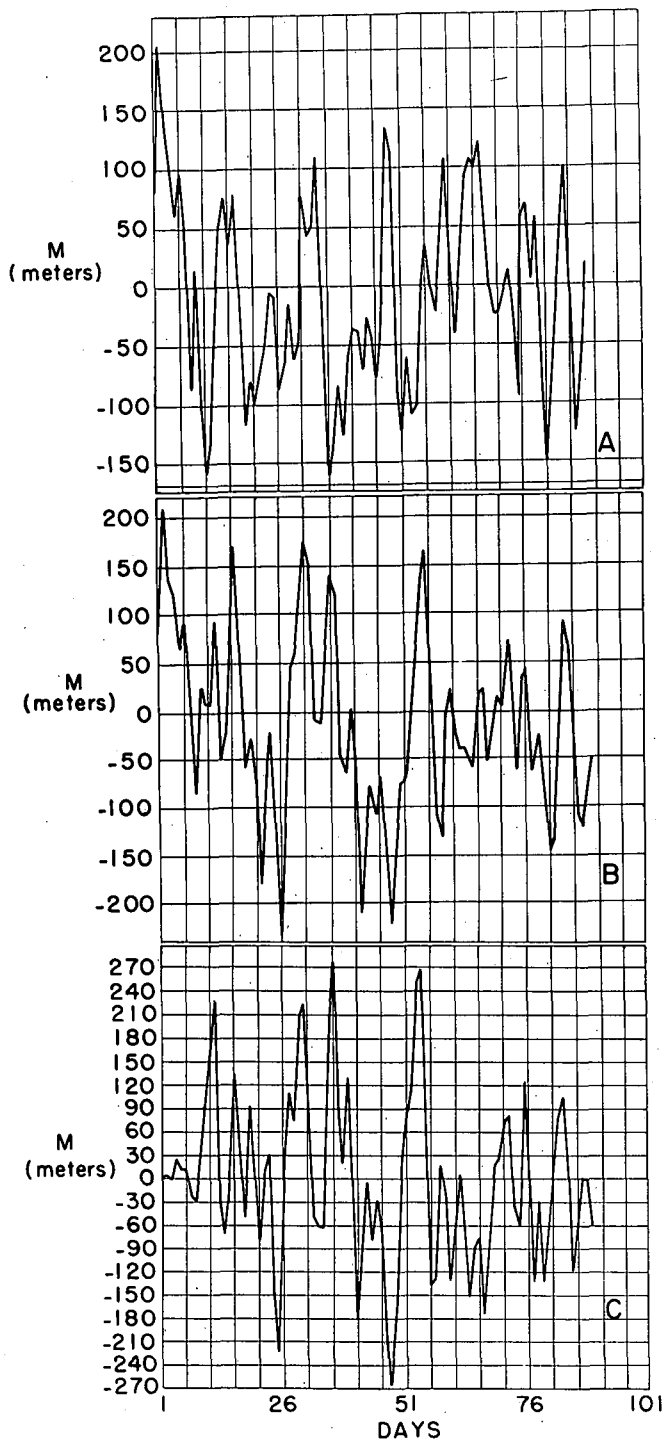


FIGURE 6.—Same as figure 4 for the 600-mb regional meridional index, M (m).

the hydrostatic effect of an augmented meridional temperature gradient on the slope of the 600-mb surface is subsequently overwhelmed by synoptic activity in the winter season.

The M -index time series (fig. 6) also fail to reveal any systematic differences between anomaly and control runs. However, power spectra of M (not shown), like those of Z , reveal consistently greater variances over all frequencies for the anomaly series than for the control. Thus, while the SST anomaly appears to have little

effect on the variance of the sea-level pressures, it does appear to increase the variances of both 600-mb circulation indices, but with little or no change in their spectral distribution.

SHTA

If the transequatorial reaction to the North Pacific SST anomaly previously noted is representative of nature, it is obviously of considerable significance for the development of long-range weather forecasting. It suggests, for example, that SST anomalies in the Southern Hemisphere, for which a satellite monitoring capability now exists (Rao et al. 1972), may be responsible for major atmospheric reactions in the Northern Hemisphere. In the SHTA experiment, the SST anomaly described previously was, in fact, placed in the South Pacific Ocean during the Southern Hemisphere winter season. The principal purpose of this experiment was to determine if an interhemispheric response similar to that computed in the NHTA-W experiment would appear in the Northern Hemisphere.

The global response to the SHTA is illustrated in figure 7 in the form of the 30-day mean sea-level pressure difference maps (anomaly minus control) for the 3-mo period. In the first month (fig. 7A), the pressure differences are everywhere small and unsystematic, not unlike those of the first month of the NHTA-W experiment. During the second month (fig. 7B), the main transequatorial effect is found in the North Atlantic Ocean. There, the displacement of an east coastal Low from Nova Scotia to Florida and the intensification of a Greenland anticyclone are reflected in positive pressure differences in excess of 10 mb between anomaly and control. This effect vanishes almost completely in the last month of the period (fig. 7C), however, when the 30-day mean pressure differences are seen to be nearly zero throughout the Northern Hemisphere. In the Southern Hemisphere, on the other hand, large pressure differences persist into the last month, notably in the South Pacific Ocean.

Further evidence of the propagation of influence across the Equator is shown in the three index difference curves in figure 8. All three indices, but most clearly the M -index (fig. 8C), indicate little or no response to the SHTA in the Northern Hemisphere during the first month. Then, abruptly, the influence of the SST anomaly arrives, and the zonal index (fig. 8B) falls while the meridional index (fig. 8C) rises relative to the control. This change in the Northern Hemisphere regional circulation at 600 mb is accompanied by a corresponding reaction in the sea-level pressure field, as shown by the pressure index, P (fig. 8A). However, the Northern Hemisphere regional response to the SHTA, like that of the total sea-level pressure field in the Northern Hemisphere, is limited to approximately the midmonth of the season. During the last quarter, the differences between anomaly and control indices return to near-zero values despite the persistence of the SST anomaly throughout the 90-day period.

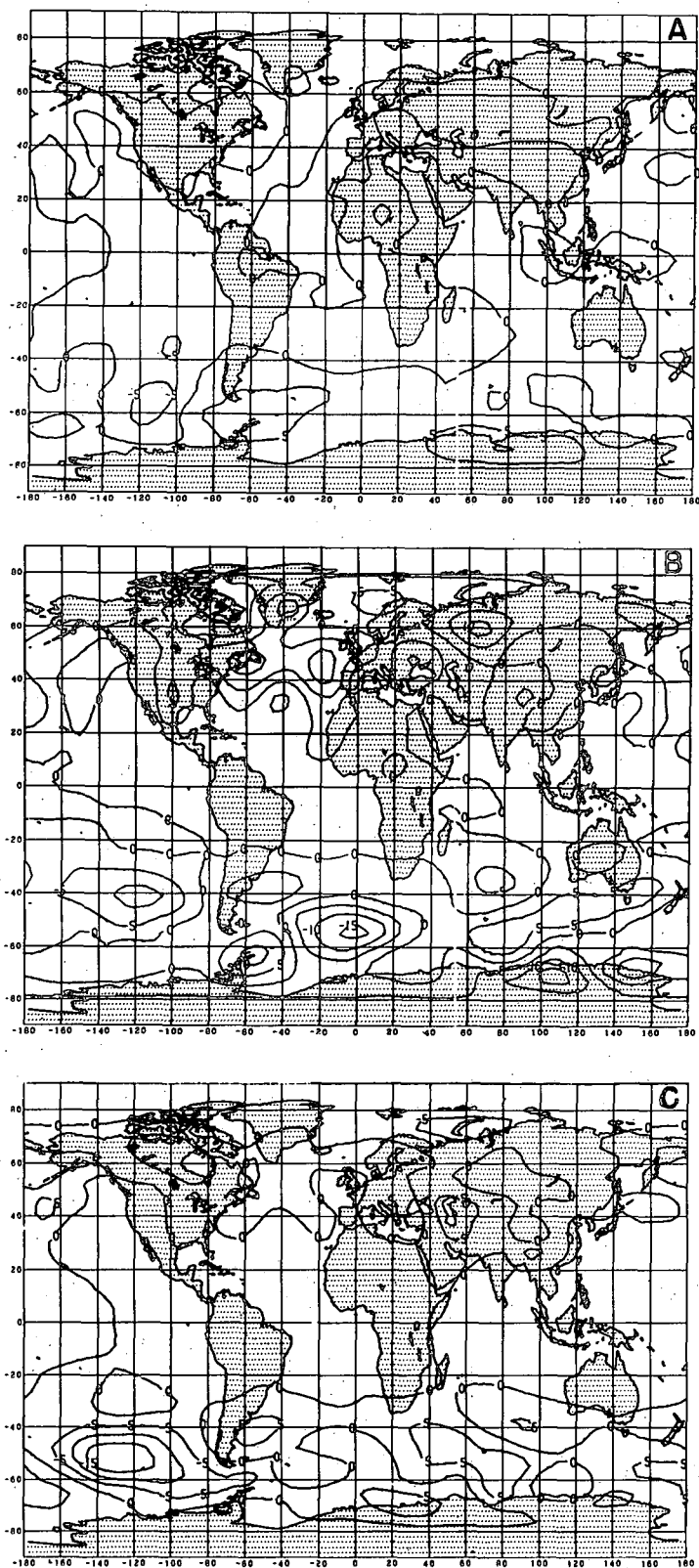


FIGURE 7.—Thirty-day mean sea-level pressure difference maps (anomaly minus control) for experiment SHTA for (A) month number 1 (1-30 days), (B) month number 2 (31-60 days), and (C) month number 3 (61-90 days).

SNW

In both SNW experiments (SNW-N and SNW-S), the most obvious effects on the 30-day mean sea-level pressure

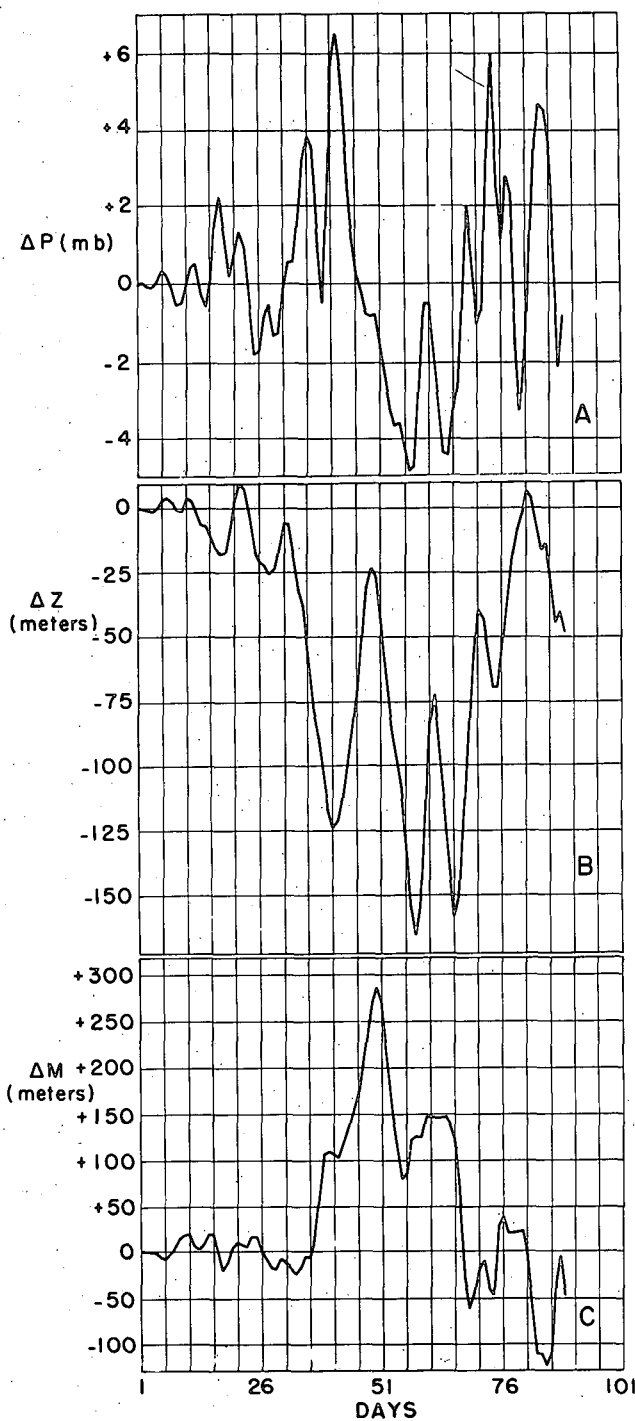


FIGURE 8.—Time series of differences (anomaly minus control) between Northern Hemisphere regional indices for experiment SHTA for (A) P (mb), (B) Z (m), and (C) M (m).

field appear in the North Atlantic region, reflecting the influence of the continental snow line on the winter monsoonal pressure differences between continents and oceans. (The monsoonal effect is much weaker in the North Pacific Ocean, presumably because of the greater size of that body.) The pressure difference fields for each of the 3 mo are shown in figures 9 and 10 for SNW-N and SNW-S, respectively. (The corresponding control pressure fields are those of figs. 1A, 2A, 3A.)

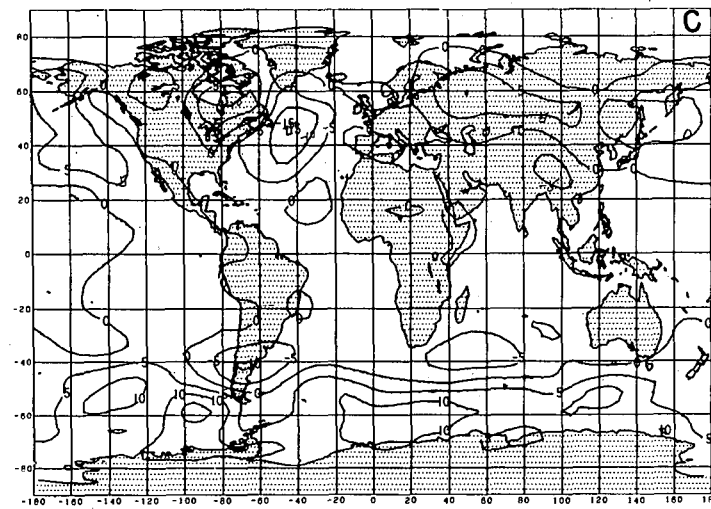
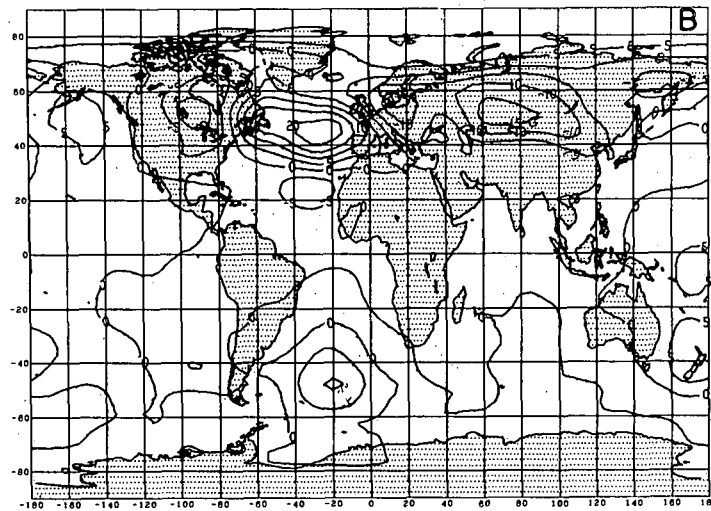
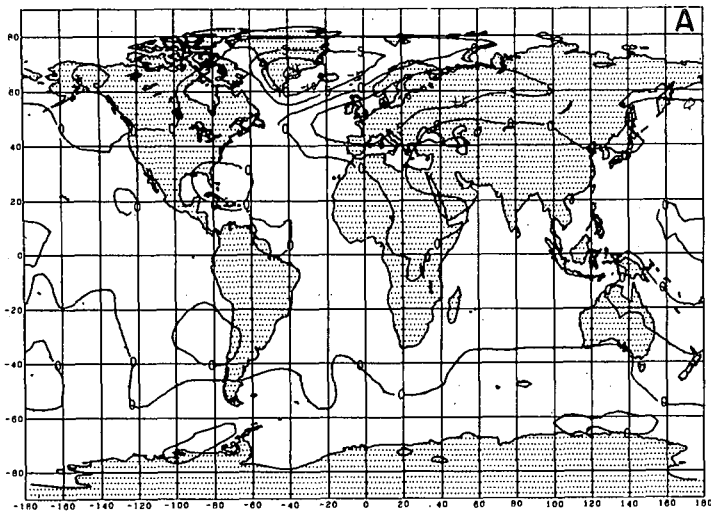


FIGURE 9.—Same as figure 7 for experiment SNW-N.

During the first month, the northward shift of the snow line (fig. 9A) is accompanied by a northward movement of the Atlantic-European trough and a weakening of the North Atlantic cyclone, while the southward shift of the snow line (fig. 10A) produces little or no effect. The difference between SNW-N and SNW-S is, however, much

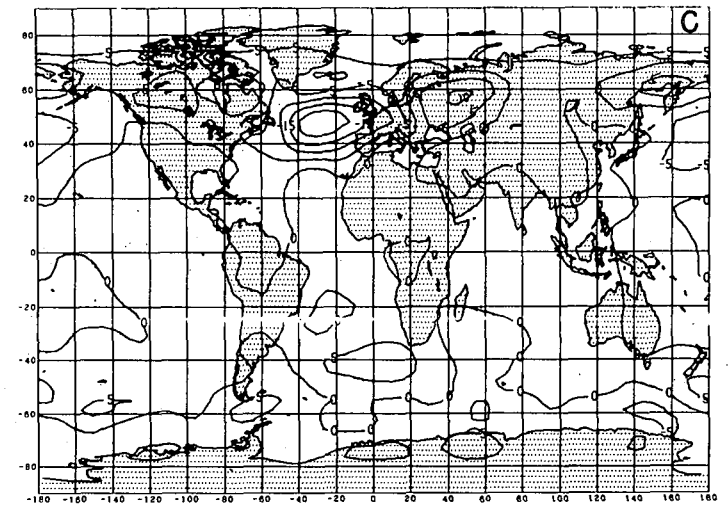
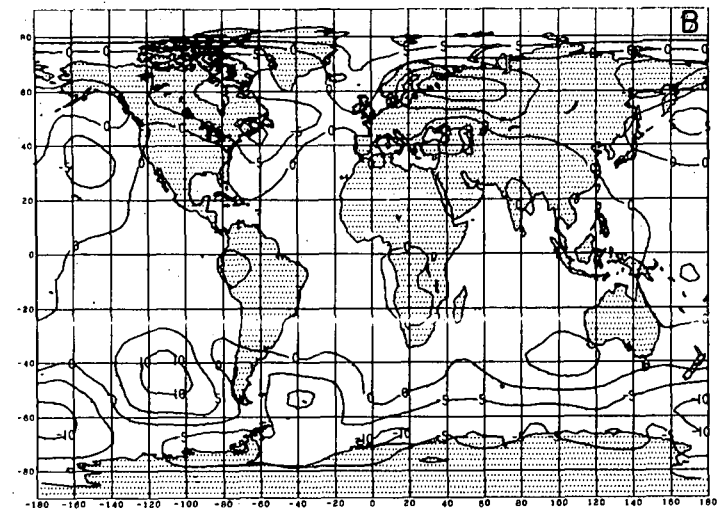
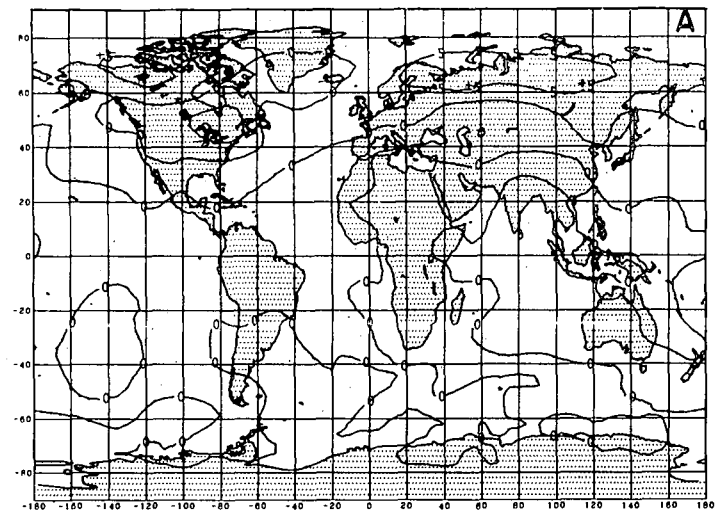


FIGURE 10.—Same as figure 7 for experiment SNW-S.

more apparent in the second month. In the former case, illustrated in figure 9B, the large, positive pressure difference in the North Atlantic represents the almost complete disappearance of the North Atlantic Low (see fig. 2A), while, in the latter case (fig. 10B), both the North Atlantic and North Pacific cyclones are deeper than those on the

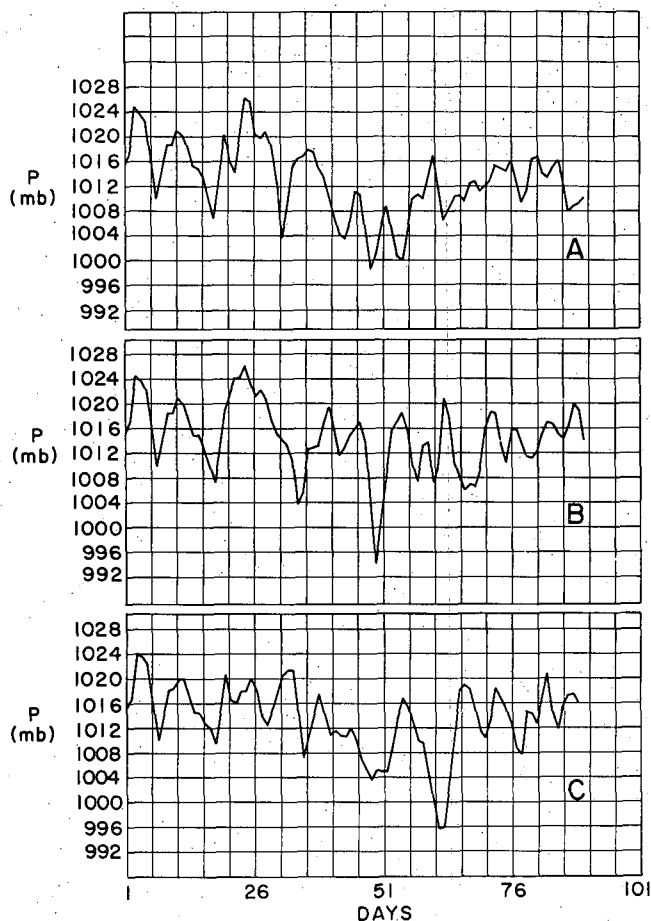


FIGURE 11.—Ninety-day time series of P-index for (A) SNW-N, (B) winter control, and (C) SNW-S.

control map. Thus, as might have been anticipated, a southward shift of the snow line enhances the monsoonal pressure difference between continent and ocean, while a northward shift tends to weaken it. Intensification of the monsoonal pressure difference associated with SNW-S persists into the third month, as shown by the large negative pressure difference in the North Atlantic Ocean in figure 10C. However, the reverse effect is not found in the third month of SNW-N. Instead, as shown by the negative pressure differences in figure 9C, the North Atlantic cyclone is restored and even intensified relative to the control in the third month of SNW-N. Nevertheless, the pressure difference between the continents and oceans is still greater for SNW-S than for SNW-N in all 3 mo.

The influence of the continental snow line on the east coastal pressure index, P , is illustrated in figure 11, showing the time series for both SNW-N and SNW-S, together with that of the control case. The outstanding effect of the snow line shift is the alteration of the major cyclonic event of 994 mb, which occurs on day 49 in the control run. In SNW-N, this event is much weaker (999 mb) and begins and ends more gradually, possibly as a result of the weaker baroclinicity associated with a more northerly snow line. The SNW-S series, on the other hand, while exhibiting a slight decrease in intensity of this event (996 mb), also shows a marked phase retardation,

with the minimum occurring 13 days later than in the control run.

5. SUMMARY AND CONCLUSIONS

The experimental results described in this paper could hardly have been anticipated in quantitative detail. They indicate how difficult it is to estimate reliably, on the basis of qualitative reasoning alone, the meteorological consequences of even the simplest alterations in surface conditions. Of course, the results of model calculations cannot be regarded as necessarily true for the real atmosphere. It is unlikely, however, that the solutions of the atmosphere will be less complicated than those of the model.

From the viewpoint of long-range weather prediction, the following results of the model experiments appear to be noteworthy:

1. The large-scale dynamical response of the atmosphere to anomalous sea-surface temperatures is generally slower, weaker, and less systematic in summer than in winter.
2. Pressure effects of sea-surface temperature anomalies propagate across the Equator after a period of about 1 mo, with no visible effects on the sea-level pressures near the Equator itself. Trans-equatorial effects are not symmetrical for the two hemispheres.
3. Neither snow line nor sea-surface temperature anomalies alter the spectral distribution of any of the indices of synoptic activity in a systematic and unambiguous manner.
4. Marked changes in the time of occurrence of major meteorological events, including phase shifts of 1-2 weeks for deep cyclones, may be induced by both SST anomalies and snow line alterations.
5. The effect of snow line shifts on the winter monsoonal land-sea pressure difference is most apparent in the North Atlantic Ocean.
6. Thirty-day mean sea-level pressure maps reveal systematic, area-limited, and relatively noise-free patterns of influence of SST and snow line anomalies.

ACKNOWLEDGMENTS

The author gratefully acknowledges the hospitality and services provided by Robert Jastrow and the staff of the Goddard Institute for Space Studies (GISS), without which this work would not have been possible. The cooperation and assistance of Milton Halem, who arranged for computing facilities, and of John Liu, who was responsible for all the programming and computations carried out for the project on a GISS computer, are especially appreciated. We also wish to thank Yale Mintz and Akio Arakawa of the University of California, Los Angeles, for graciously allowing us to use their model and programs for these experiments. Shu-hsien Chow performed the spectral analyses and contributed to the study of the SNW experiment at New York University.

REFERENCES

- Arakawa, Akio, Katayama, Akira, and Mintz, Yale, "Numerical Simulation of the General Circulation of the Atmosphere," *Proceedings of the WMO/IUGG Symposium on Numerical Weather Prediction, Tokyo, Japan, November 26-December 4, 1968*, Japan Meteorological Agency, Tokyo, Mar. 1969, pp. IV-7 to IV-8-12.
- Bjerknes, Jakob A., "A Possible Response of the Atmospheric Hadley Circulation to Equatorial Anomalies of Ocean Temperature," *Tellus*, Vol. 18, No. 4, Stockholm, Sweden, 1966, pp. 820-829.
- Bjerknes, Jakob A., "Atmospheric Teleconnections From the Equatorial Pacific," *Monthly Weather Review*, Vol. 97, No. 3, Mar. 1969, pp. 163-172.

- Gates, W. L., Batten, E. S., Kahle, A. B., and Nelson, A. B., "A Documentation of the Mintz-Arakawa Two-Level Atmospheric General Circulation Model," *Report No. R-877-ARPA*, The RAND Corporation, Santa Monica, Calif., Dec. 1971, 408 pp.
- Holloway, J. Leith, Jr., and Manabe, Syukuro, "Simulation of Climate by a Global General Circulation Model," *Monthly Weather Review*, Vol. 99, No. 5, May 1971, pp. 335-370.
- Kasahara, Akira, and Washington, Warren M., "NCAR Global General Circulation Model of the Atmosphere," *Monthly Weather Review*, Vol. 95, No. 7, July 1967, pp. 389-402.
- Langlois, W. E., and Kwok, H. C. W., "Description of the Mintz-Arakawa Numerical General Circulation Model," *Technical Report No. 3, Numerical Simulation of Weather and Climate*, Department of Meteorology, University of California, Los Angeles, Feb. 1969, 95 pp.
- Leith, Cecil E., "Numerical Simulation of the Earth's Atmosphere," *Methods in Computational Physics*, Vol. 4, Academic Press, New York 1965, pp. 1-28.
- Manabe, Syukuro, and Bryan, Kirk, "Climate Calculations With a Combined Ocean-Atmosphere Model," *Journal of the Atmospheric Sciences*, Vol. 26, No. 4, July 1969, pp. 786-789.
- Mintz, Yale, "Very Long-Term Global Integration of the Primitive Equations of Atmospheric Motion," *WMO Technical Note No. 66*, World Meteorological Organization, Geneva, Switzerland, 1965, pp. 141-167.
- Mintz, Yale, Katayama, Akira, and Arakawa, Akio, "Numerical Simulation of the Seasonally and Inter-Annually Varying Tropospheric Circulation," *Climatic Impact Assessment Program, Proceedings of the Survey Conference, Cambridge, Massachusetts, February 15-16, 1972*, Report No. DOT-TSC-OST-72-13, U.S. Department of Transportation, Washington, D.C., Sept. 1972, pp. 194-216.
- Namias, Jerome, "Influences of Abnormal Surface Heat Sources and Sinks on Atmospheric Behavior," *Proceedings of the International Symposium on Numerical Weather Prediction, Tokyo, Japan, November 7-13, 1960*, Meteorological Society of Japan, Tokyo, Mar. 1962, pp. 615-627, 656 pp.
- Namias, Jerome, "Seasonal Interactions Between the North Pacific Ocean and the Atmosphere During the 1960's," *Monthly Weather Review*, Vol. 97, No. 3, Mar. 1969, pp. 173-192.
- Namias, Jerome, "Macroscale Variations in Sea-Surface Temperatures in the North Pacific," *Journal of Geophysical Research*, Vol. 75, No. 3, Jan. 20, 1970, pp. 565-582.
- Namias, Jerome, "The 1968-69 Winter as an Outgrowth of Sea and Air Coupling During Antecedent Seasons," *Journal of Physical Oceanography*, Vol. 1, No. 2, Apr. 1971, pp. 65-81.
- National Academy of Sciences, "The Feasibility of a Global Observation and Analysis Experiment," Report of the Panel on International Meteorological Cooperation to the Committee on Atmospheric Sciences, National Academy of Sciences, National Research Council, Publication 1290, National Academy of Sciences-National Research Council, Washington, D.C., 1966, 172 pp.
- Rao, P. Krishna, Smith, W. L., and Koffler, R., "Global Sea-Surface Temperature Distribution Determined From an Environmental Satellite," *Monthly Weather Review*, Vol. 100, No. 1, Jan. 1972, pp. 10-14.
- Rowntree, P. R., "The Influence of Tropical East Pacific Ocean Temperatures on the Atmosphere," *Quarterly Journal of the Royal Meteorological Society*, Vol. 98, No. 416, Apr. 1972, pp. 290-321.
- Smagorinsky, Joseph, Manabe, Syukuro, and Holloway, J. Leith Jr., "Numerical Results From a Nine-Level General Circulation Model of the Atmosphere," *Monthly Weather Review*, Vol. 93, No. 12, Dec. 1965, pp. 727-768.
- Spar, Jerome, "Effects of Surface Anomalies on Certain Model-Generated Meteorological Histories," New York University, Geophysical Sciences Laboratory *Interim Report No. GSL-TR-72-2*, Apr. 1972, 54 pp.

[Received June 15, 1972; revised August 27, 1972]